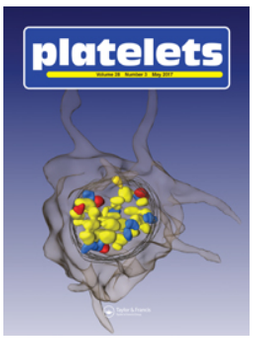

Platelets

ISSN: 0953-7104 (Print) 1369-1635 (Online) Journal homepage: http://www.tandfonline.com/loi/iplt20

Extracellular vesicles from activated platelets: a semiquantitative cryo-electron microscopy and immuno-gold labeling study

Alain R. Brisson, Sisareuth Tan, Romain Linares, Céline Gounou & Nicolas Arraud

To cite this article: Alain R. Brisson, Sisareuth Tan, Romain Linares, Céline Gounou & Nicolas Arraud (2017) Extracellular vesicles from activated platelets: a semiquantitative cryo-electron microscopy and immuno-gold labeling study, Platelets, 28:3, 263-271, DOI: 10.1080/09537104.2016.1268255

To link to this article: http://dx.doi.org/10.1080/09537104.2016.1268255

Published online: 19 Jan 2017.

platelets

http://www.tandfonline.com/iplt
ISSN: 0953-7104 (print), 1369-1635 (electronic)

Platelets, 2017; 28(3): 263–271
 DOI: 10.1080/09537104.2016.1268255

Taylor & Francis
Taylor & Francis Group

SPECIAL PAPER: PLATELET MICROVESICLES

Extracellular vesicles from activated platelets: a semiquantitative cryo-electron microscopy and immuno-gold labeling study

Alain R. Brisson, Sisareuth Tan, Romain Linares, Céline Gounou, & Nicolas Arraud*

Extracellular Vesicles and Membrane Repair, UMR-5248-CBMN CNRS-University of Bordeaux-IPB, Allée Geoffroy Saint-Hilaire, Pessac, France

ABSTRACT

Cells release membrane vesicles in their surrounding medium either constitutively or in response to activating signals. Two main types of extracellular vesicles (EVs) are commonly distinguished based on their mechanism of formation, membrane composition and size. According to the current model, EVs shed from the plasma membrane, often called microvesicles, expose phosphatidylserine (PS) and range in size from 100 nm to 1 μm, while EVs originating from endosomal multi-vesicular bodies, called exosomes, contain tetraspanin proteins, including CD63, and range in size from 50 to 100 nm. Heijnen et al. [1] have shown that activated platelets release EVs corresponding to these two types of vesicles, using negative staining electron microscopy (EM) and immuno-gold labeling. Here, we apply cryo-EM and immuno-gold labeling to provide a quantitative analysis of EVs released by platelets activated by thrombin, TRAP and CRP-XL, as well as EVs from serum. We show that EVs activated by these three agonists present a similar size distribution, the majority of them forming a broad peak extending from 50 nm to 1 μm, about 50% of them ranging from 50 to 400 nm. We show also that 60% of the EVs from TRAP or CRP-XL activation expose CD41, a majority of them exposing also PS. To explain the presence of large EVs CD41-negative or PS-negative, several alternative mechanisms of EV formation are proposed. We find also that the majority of EVs in activated platelet samples expose CD63, and distinguish two populations of CD63-positive EVs, namely large EVs with low labeling density and small EVs with high labeling density.

Keywords

Annexin-A5, CD41, CD63, cryo-transmission electron microscopy, extracellular vesicles, immuno-gold labeling, phosphatidylserine exposure, platelets

History

Received 26 October 2016
Revised 23 November 2016
Accepted 24 November 2016
Published online 18 January 2017

Introduction

Cells respond to a variety of stimuli by releasing membrane vesicles in their surrounding medium [2]. Two main types of cell-derived vesicles are commonly distinguished depending on their mechanism of formation. One type of vesicles, called microparticles or microvesicles, consists of small pieces of the cell plasma membrane shed into the extracellular medium. This process involves a profound membrane reorganization characterized by a loss of phospholipid asymmetry and the exposure of phosphatidylserine (PS) molecules on the outer membrane leaflet, conferring pro-coagulant properties to shed vesicles [3, 4]. Exosomes, the second type of cell-derived vesicles, are contained in multi-vesicular bodies and secreted by cells after fusion of this endosomal compartment with the plasma membrane [5]. It is commonly considered that these two types of vesicles differ by their size, from 100 nm to 1 μm for microvesicles versus from 50 to 100 nm for exosomes [6]. However, an objective distinction between these vesicles is hampered by the lack of reliable methods of characterization and separation; thus, the term extracellular vesicle (EV) will be used here collectively for designing all types of membrane vesicles released by cells [7].

The interest in EVs has grown considerably over the last two decades, resulting in an abundant literature describing the presence of EVs and their direct participation in health and disease situations [8–11]. In addition, intense research focuses on the potential applications of EVs as disease biomarkers [12]. However, the heterogeneity of EVs, in cell origin, composition, size, properties and functions, and the lack of methods allowing their detailed analysis make our current knowledge on EVs still limited.

Blood, the major body fluid, contains EVs released by all cell types from the vascular system, and potentially EVs from other tissues collected from blood circulation. While it is commonly considered that EVs from red blood cells and platelets are predominant, a consensus on their absolute concentrations is lacking, with reported values for total EV concentrations varying from 200 to 10^9 per μL plasma [13]. Our group has recently pioneered an approach combining cryo-transmission electron microscopy (cryo-EM), immuno-gold labeling and fluorescence-triggered flow cytometry with the objective of providing a comprehensive description of EVs in plasma [14–16]. This work, performed on platelet-free plasma (PFP) samples from healthy donors, led to several major results concerning the morphology, the size distribution and the relative concentrations of the main EV populations, namely PS-exposing EVs and EVs derived from platelets and erythrocytes. Noticeably, we found that, in contrast to the classical theory of EV formation, about half of the EVs were not labeled by Annexin-A5 (Anx5), a high-affinity ligand of PS-exposing membranes [17].

The objective of the present study was to extend this initial analysis by addressing the same basic questions on EVs'

*Current affiliation: Flow Cytometry Laboratory, Hematology and Clinical Pathology Services, HUG, Geneva, Switzerland.

Correspondence: Alain R. Brisson, UMR-5248-CBMN, Bat. B14, Allée Geoffroy Saint-Hilaire, F-33600, Pessac, France. E-mail: a.brisson@cbmn.u-bordeaux.fr

morphology, size distribution, PS exposure and phenotype at the level of activated platelets.

Platelet EVs were discovered by Wolf [18], who described the formation of 'platelet-dust' particles upon platelet activation, and proposed their role in blood coagulation [18, 19]. Platelet-derived EVs have since been the subject of many studies [20] and proposed to participate in a variety of pathological disorders [11, 21], 22]. It is now well established that the pro-coagulant activity of activated platelets is due to the exposure of PS on the outer leaflet of the platelet plasma membrane [23] and that changes in phospholipid distribution are accompanied by the shedding of vesicles from the platelet plasma membrane [24]. Flow cytometry [24, 25] and EM [1, 26] studies have shown that platelet EVs expose PS, thus providing pro-coagulant surfaces. Heijnen et al. [1] have shown by immune-EM that activated platelets release two distinct types of vesicles, namely plasma membrane-derived microvesicles and multi-vesicular body-derived exosomes. In this study, microvesicles and exosomes were separated by differential centrifugation and microvesicles were identified based on their PS exposure via specific labeling with Anx5-conjugated gold particles, while exosomes were identified by immuno-gold labeling of CD63, a tetraspanin enriched in multi-vesicular bodies and a classical marker of exosomes [27, 28]. The objective of the present study is to provide a quantitative analysis of these two types of EVs from platelets activated with thrombin, TRAP or CRP-XL and serum samples, using cryo-EM and immuno-gold labeling techniques.

Material and methods

1- Material

Human α-thrombin and PPACK (Phe-Pro-Arg-chloromethylketone) were from Cryopep (Montpellier, France). Thrombin receptor activating peptide (TRAP) was a gift from Dr. Nurden (CHU Bordeaux). Cross-linked collagen-related peptide (CRP-XL) was obtained from Dr. Farndale (Cambridge University). Annexin-5 was produced and conjugated to cyanine-5 (Cy5) as described in Bouter et al. (2011). Anti-CD41 monoclonal antibody (mAb) (clone P2) and anti-CD63 mAb (clone H5C6) were from Beckman Coulter (Villepinte, France) and BD Biosciences (Le Pont de Clay, France), respectively. Anti-CD41-mAb-PE was from Beckman Coulter. All other chemicals were of ultrapure grade. Water was purified with a RiOs system (Millipore, France).

2- Preparation of activated platelets

Blood was collected from four healthy adult donors after written informed consent. Peripheral blood was collected in 4.5 mL BD Vacutainer® tubes containing 0.1 volume 105 mM sodium citrate. Platelet-rich plasma (PRP) was obtained by centrifugation at 200 g for 10 min at 20–24°C, less than one hour after blood collection. The upper half of the supernatant was harvested and pooled, giving PRP samples containing 5–7 × 10^5 platelets/μL. For serum samples, blood was collected in 3.5 mL BD Vacutainer® SST-II-Advance tubes. After centrifugation at 1,800 g for 10 min, 1 mL serum was withdrawn from the supernatant.

For each PRP sample, platelets were activated as follows. Aliquots of 100 μL freshly prepared PRP were diluted 2× with Tyrode buffer supplemented with 10 μM PPACK and 2 mM $CaCl_2$ and incubated for 1 h with 0.5 U/mL thrombin, 12.5 μg/mL TRAP or 1 μg/mL CRP-XL.

3- Immuno-gold labeling and cryo-EM

Gold nanoparticles (NPs) were conjugated with Anx5 and with anti-CD41 or anti-CD63 mAbs following procedures previously described [14]. Freshly activated platelets were diluted 100×with a HEPES-buffered saline (HBS) containing 150 mM NaCl, 2 mM $CaCl_2$ and 10 mM HEPES, pH 7.4, and labeled successively for 1 h with 1–4 × 10^{15} gold-NP/L 10-nm anti-CD41- or anti-CD63-gold-NP, then for 30 min with 1–4 × 10^{15} NP/L 4-nm Anx5-gold-NP. Immuno-gold labeled samples were processed for cryo-EM as follows. A 4-μL aliquot was deposited on an EM grid coated with a perforated carbon film; the liquid was blotted from the backside of the grid and the grid was quickly plunged into liquid ethane using a Leica EMCPC cryo-chamber. EM grids were stored under liquid nitrogen prior to EM observation. Cryo-EM was performed with a Tecnai F20 (FEI, USA) microscope equipped with a USC1000-SSCCD camera (Gatan, USA).

4- Flow cytometry

Nonactivated and activated PRP samples were labeled with Anx5-Cy5 and anti-CD41-mAb-PE as follows. For Anx5 labeling, PRP samples were diluted 300× with HBS supplemented with 10 μM PPACK, then 20 ng/mL Anx5-Cy5 was added and incubated for 45 min at room temperature in the dark. For labeling with anti-CD41-mAb-PE, 10 μL PRP samples were diluted 6× with HBS, anti-CD41-mAb-PE (final dilution 50x) was added and incubated for 2 h, and then the mixture was diluted 50×with HBS before FCM analysis [16]. Flow cytometry was performed with a Gallios flow cytometer (Beckman Coulter), using settings described in [16]. Flow cytometry measurements were performed with triggering based on light scattering intensity and on fluorescence intensity, as described in details in [16].

Results

1- Flow cytometry of activated platelets

Platelet activation of freshly prepared PRP samples was induced with thrombin, TRAP or CRP-XL, as described in Methods section. The effect of these agonists was first evaluated by flow cytometry. The overall structural changes of platelets were determined by measuring the forward scatter (FS) and side scatter (SS) intensity, while the exposure of PS was determined by Anx5-Cy5 labeling. Figure 1 shows the results obtained for CRP-XL activation. Basically, after agonist addition, the cluster of platelets (contained in the platelet gate) was observed to shift toward lower FS and SS values, forming a continuum of events, which extends downward outside the platelet gate, mixed with the noise [29, 30]. In addition, the number of PS-exposing EVs, identified as events of low FS versus SS values labeled by Anx5-Cy5, was found to increase strongly after activation.

In the conditions of activation used here, we found that CRP-XL was the most efficient agonist (Figure 1C). The large increase in the number of PS-positive EVs in activated PRP samples, namely up to 100× for CRP-XL, indicates that the vast majority of EVs derive from platelets. This justifies our choice to perform the following cryo-EM study on PRP samples and not on washed platelets.

2- Immuno-cryo-EM analysis of EVs from activated platelets

2-1 Morphology and size distribution of EVs

Compared with our initial cryo-EM study, which was performed on pure PFP samples [14], the number of EVs observed here in 100× diluted activated PRP samples was significantly higher, which facilitated the analysis considerably. This further indicates that endogenous EVs, that is, EVs present in PRP before activation, constitute a negligible part of EVs in activated PRP. For each condition, several hundred cryo-EM images were recorded, from which about 1,000 EVs were identified and analyzed for their morphology, size and phenotype.

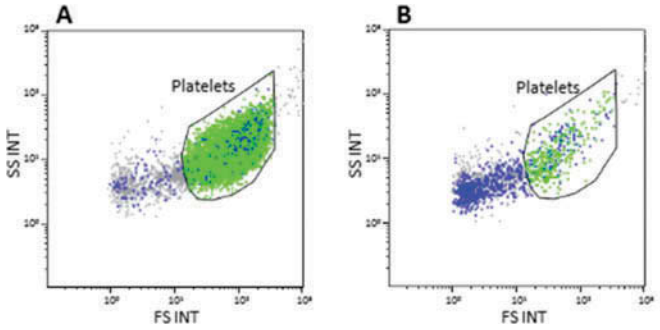

C

	EV / µL
PRP	31 013
+ Thrombin	414 216
+ TRAP	284 719
+ CRP-XL	3 592 879

Figure 1. Flow cytometry analysis of activated platelets. Typical dot plots of side scatter intensity (SS INT) versus forward scatter intensity (FS INT) of a fresh PRP sample before (A) and after activation for 1 h with 1 µg/mL CRP-XL. Events labeled by Anx5-Cy5 are colored blue. The platelet gate contains all the events (colored green) forming a cluster of high SS versus FS values labeled with anti-CD41-mAb-PE. Events colored grey correspond to the scattering noise from the buffer.(C) Number of Anx5-positive EVs in a PRP sample before and after activation with thrombin, TRAP or CRP-XL as described in Methods section. EV numbers were measured by fluorescence triggering [32].

The main type of EVs present in activated platelets consisted of isolated spherical EVs, of diameter ranging from 50 nm to 1 µm (Figure 2A–C). The second largest type of EVs consisted of clusters of EVs, made of the tight association of spherical EVs (Figure 2D). A cluster is defined here as an association of at least three EVs. The number of EVs per cluster was highly variable, the majority of clusters comprising between 5 and 10 EVs and being larger than 1 µm. It must be stressed that, over a decade of analysis of PFP samples from healthy donors, we observed exclusively isolated EVs and no EV clusters (Arraud et al. [14]). We conclude therefore that the EV clusters observed in activated platelets are genuine objects, which do not result from an artifact of cryo-EM preparation. In addition to isolated spherical EVs and EV clusters, low amounts of EVs of tubular morphology (200–500 nm in diameter and 1–10 µm in length) (Figure 2E), and large platelet fragments measuring from 1 to several µm (Figure 2F) are also present in activated platelet samples. The presence of tubular EVs was highly dependent on the agonist used, being maximal for 1 h TRAP activation. Most tubes contain internal striations, which are more or less visible depending on imaging conditions (Figure 2E). Finally, a large number of platelets were also present on EM grids (data not shown), as expected because no treatment was applied to eliminate them.

Serum samples presented a similar EV composition, consisting of isolated EVs, EV clusters and large fragments (data not shown). Platelets were almost entirely absent from serum samples, as expected from clotted blood and from the presence of a separating gel acting as a filter retaining aggregated platelets in serum collection tubes.

The size distribution of EVs from activated platelets is similar for the three agonists (Figure 3). A broad peak extending from 50 nm to 1 µm contains about 80% of EVs, about 50% of them ranging from 50 to 400 nm. Objects larger than 1 µm, consisting of tubular EVs and large fragments, form a second peak, accounting for about 15% of all EVs.

The size distribution of EVs from serum is similar to that observed with the three agonists, with 80% EVs ranging from 50 nm to 1 µm. However, EVs ranging from 400 to 600 nm are more abundant in the serum, forming about 30% of EVs (data not shown).

2-2 Phenotype of EVs released by activated platelets

Next, we focused on the population of EVs originating from the plasma membrane, as well as the population of EVs exposing PS. Indeed, according to classical theory, platelet activation leads to the release of plasma membrane vesicles exposing PS on their outer surface [3]. Gold-NPs conjugated to an anti-CD41-mAb were synthesized to label the $\alpha_{IIb}\beta_3$ integrin, the most abundant platelet surface membrane glycoprotein [31], and gold-NPs conjugated to Anx5 were used to label PS-exposing membranes. This analysis was limited to TRAP and CRP-XL activation, because the results obtained with thrombin were poorly reproducible.

We found that about 60% of EVs released by platelets after TRAP or CRP-XL activation expose CD41 (Figure 4A). The majority of them, namely about 80% for TRAP and 90% for CRP-XL, were PS-positive. With CRP-XL activation, the majority of EVs larger than 500 nm, including EV clusters and fragments, expose both CD41 and PS (CD41+/PS+) (Figure 4B). With TRAP activation, the same result is observed, with the exception of the long tubular EVs (Figure 2E), which are almost all CD41+/PS- (Figure 4C). With both agonists, CD41-/PS- and CD41-/PS+ EVs amounted to about 20% of the total EVs, each (Figure 4A). These populations corresponded mainly to EVs of small size, about 90% of them being smaller than 300 nm for CD41-/PS- EVs and 500 nm for CD41-/PS+ EVs (Figure 4B,C).

The situation was found to be markedly different with serum samples. Nearly 90% EVs are CD41+, among which nearly 100% are PS+ (Figure 4A). About 10% EVs are CD41-/PS-, and correspond to EVs smaller than 200 nm (data not shown).

We observed that the density of CD41 labeling was not homogeneous between platelets or between areas within a given platelet, some platelets being significantly more labeled than others (Figure 5). In particular, platelet pseudopods presented a high-density labeling. This result, not reported earlier to our knowledge, indicates either an increased affinity of the anti-CD41-mAb for its receptor after activation or a higher density of CD41 locally, in areas where platelet activation takes place, like the pseudopods. The well-known conformational change of the $\alpha_{IIb}\beta_3$ integrin upon platelet activation (Shattil, Kim, et Ginsberg 2010; Kahner et al. 2012) supports the former hypothesis.

In this context, the number of membrane-bound gold-NPs deserves a comment. This number should not be taken as an absolute number, because the conditions of labeling do not correspond to saturation. The binding of only few gold-NPs, at least three, to an EV is considered significant because the surrounding medium contains basically no gold-NP. A simple calculation shows that, with the concentration of gold-NPs used here ($1–4 \times 10^{15}$ NP/L), a 300-nm-thick layer contains $1–4 \times 10^{-3}$ gold-NPs per μm^2, which is equivalent to about 1 gold-NP per EM grid square.

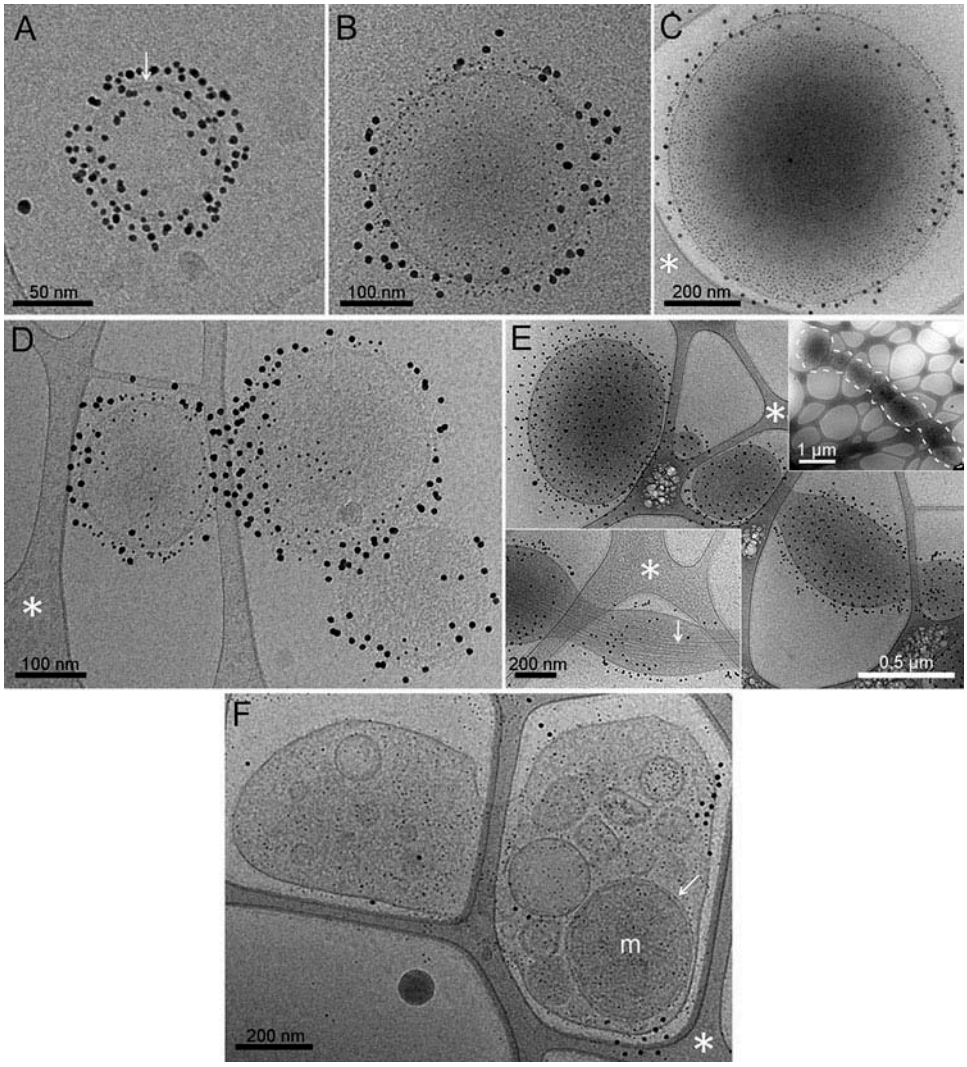

Figure 2. Morphology and size of EVs in activated platelet samples. All the images in Figures 2, 5 and 7 (except Figure 6B) were taken for double labeling experiments with 4-nm Anx5-gold-NPs and 10-nm anti-CD41-gold-NPs. In all images from Figures 2, 5, 6 and 7, the white asterisks point to areas of the carbon support film.(A–C) Typical images of isolated spherical EVs, of 90 nm, 300 nm and 750 nm diameter, respectively. The EV in (A) is single labeled by Anx5-gold-NPs while the EVs in (B) and (C) are CD41+/PS+. In (A), the two lipid leaflets of the membrane are well resolved, separated by about 4 nm (white arrow). In many EV images, e.g. (B–D), the large gold particles are localized at the vesicle periphery, while they are expected to be distributed homogeneously over the vesicle surface. Our hypothesis is that, when the liquid film thickness becomes close to the vesicle diameter, the elements close to the liquid–air interface are displaced laterally due to surface tension, relocalizing at vesicle surfaces in contact with the liquid.(D) Typical image of an EV cluster, made of the tight association of three spherical EVs, which are CD41+/Anx5+. (E) Typical images of tubular EVs observed after TRAP activation. These EVs are CD41+/Anx5, like almost all tubular EVs. (top), tubular EV of about 5.5 µm length; (înset: for clarity, the tube is surrounded by a dashed white line). (bottom), portion of a tubular EV showing long and parallel fibers (white arrow). (F) Fragment of a platelet, containing various types of membrane vesicles, including a mitochondrion (m) recognizable by its characteristic double membrane (white arrow). (A, C, F) CRP-XL activation; (B) serum; (D, E) TRAP activation.

3- CD63-exposing EVs from activated platelets

Next, we focused on the population of CD63-positive EVs. As indicated above, our objective was to provide a quantitative analysis of the two main types of activated platelet EVs, namely EVs shed from the platelet plasma membranes, characterized by their PS exposure, and referred to as microparticles or microvesicles, and EVs released from multi-vesicular bodies, characterized by their small size and the exposure of CD63, and referred to as exosomes [1]. Gold-NPs conjugated with anti-CD63-mAbs were synthesized in order to identify CD63-positive EVs.

Surprisingly, we found that most EVs in activated platelet samples were labeled with anti-CD63-gold-NPs. Two main types of CD63-positive EVs can be distinguished, depending on their labeling density and their size. The majority of them, ranging from 200 to 1 µm, consisted of EVs weakly labeled by anti-CD63-gold-NPs (Figure 6A, B). The majority of these CD63-positive EVs are also labeled by Anx5-gold-NPs, and thus expose PS. The second population of CD63-positive EVs consisted of small EVs, ranging in size from 50 to 200 nm, which were covered with a high density of anti-CD63-gold-NPs (Figure 6C-E). Some of these CD63-positive EVs were PS-positive, and others were PS-negative. Although the number of gold-NPs should not be taken in an absolute manner, a comparison of the surface density of CD63 labeling between these two types of EVs indicates that the labeling density of the small vesicles is significantly higher – by about 50 times – than that of the larger EVs. These small EVs, highly expressing CD63, correspond most likely to the so-called exosomes originating from multi-vesicular bodies [1, 27].

In serum, nearly 90% of the EVs larger than 200 nm were CD63 +/PS+. As most EVs are also CD41+/PS+ as indicated above, we conclude that the vast majority of EVs in serum are CD41+/CD63 +/PS+ and originate therefore from the plasma membrane.

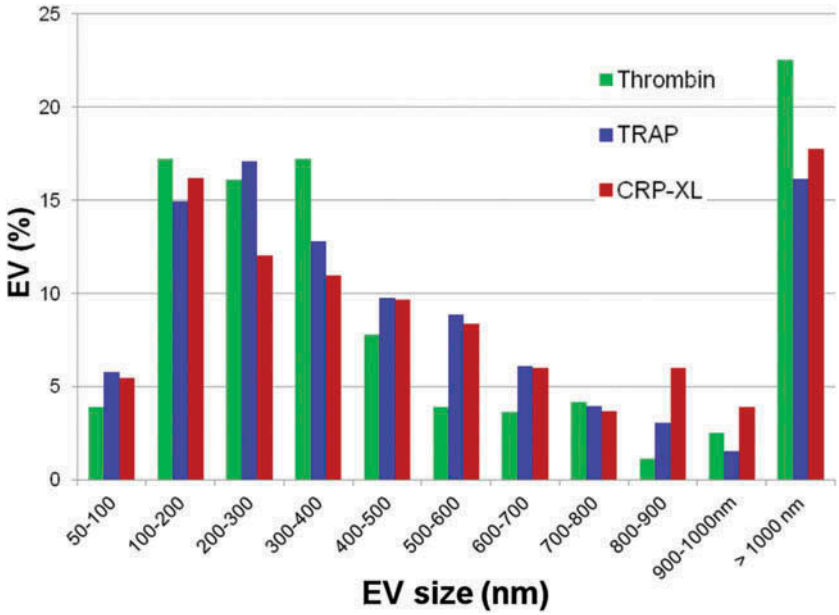

Figure 3. Size distribution of EVs from activated platelets. Size histograms of EVs observed after thrombin (green), TRAP (red) and CRP-XL (blue) activation.

Discussion

This study provides a quantitative analysis of EVs released by platelets upon activation, with a focus on their size distribution and the presence on their surface of markers, namely PS, CD41 and CD63.

This study was carried out on PRP samples and not on washed platelets for two main reasons. First, we made several preparations of washed platelets in the presence of apyrase and observed a moderate yet systematic platelet activation, the number of Anx5-positive EVs in washed platelets corresponding to about 4× the basal level measured with fresh PRP (data not shown). Second, the number of EVs obtained after activation exceeds by far the number of EVs in nonactivated PRP samples (Figure 1C). Finally, complementary experiments of immuno-gold labeling with anti-CD235a-mAb showed that EVs of erythrocyte origin represented less than 1% of the total amount of EVs in activated PRP (data not shown). Erythrocyte-derived EVs form, together with platelet-derived EVs, the main EV population in PFP [14, 32], and this confirms that endogenous EVs constitute a negligible part of EVs in activated PRP.

As indicated above, this study was possible thanks to the high signal-to-noise ratio and the all-or-none labeling situation observed for PS, CD41 and CD63, demonstrating the power of the immuno-cryo-EM approach.

Size distribution of EVs from activated platelets

A major result of this study concerns the size distribution of EVs from activated platelets. For the three agonists used here, the major EV population consists of isolated spherical EVs forming a broad peak extending from 50 nm up to about 1 μm, about 50% of them ranging from 50 to 400 nm. To our knowledge, this is the first study in which the size distribution of EVs is determined, at the single EV level, over several thousand EVs. Although EVs are commonly described as a heterogeneous population of particles ranging from 50 nm to 1 μm, this assertion has been poorly substantiated at the experimental level until now. Historically, platelet-derived EVs were described as platelet dust made up of particles 20 to 50 nm in diameter [18], and later as particles with an average diameter of 100 nm [24]. Our study demonstrates that EVs of 100 nm or smaller represent only a minority (less than 10%) of all EVs, and not a single vesicle smaller than 50 nm was found to expose either PS or CD41. It is therefore logical to ask the question of the nature of the particles described as platelet dust by Wolf [18].

More recent data on EV size were obtained by EM [1, 33], atomic force microscopy (AFM) [33, 34], dynamic light scattering (DLS) [33, 35] or nanoparticle tracking analysis (NTA) [36]. Using immuno-EM on negatively stained samples from purified fractions of activated platelet EVs, Heijnen et al. [1] reported results qualitatively close to those presented here, concluding the presence of two types of EVs, namely PS-positive microvesicles ranging from 100 nm to 1 μm, and CD63-positive exosomes ranging from 40 to 100 nm. Using DLS, Lawrie et al. [35] reported that fresh frozen plasma EVs ranged from 100 to 500 nm, which is also close to our results. On the other hand, several studies have concluded that plasma samples contain a majority of small EVs, of 40 nm [34] or 80 nm [36] peak values, which is difficult to reconcile with the results presented here and stresses the difficulty of measuring EVs and the limitations of the applied methods.

Finally, some caution must be taken regarding the sizes determined from cryo-EM images, because EVs may suffer from some flattening during the formation of a thin frozen film due to surface tension effects. At maximal flattening, a spherical EV, of radius R and area $4\pi R^2$, would transform into a circular pancake, of radius R' and area $2\pi R'^2$, so that the radius of the flattened pancake is related to the radius of the original sphere by the relationship $R = R'\sqrt{2}$. Therefore, the actual size of EVs may be overestimated by 10 or 20%, at most 40%. If present, this effect is likely to affect larger EVs more importantly than smaller ones.

About the mechanisms of EV formation

We found that about 40% of the EVs released by activated platelets do not expose CD41 and that most of these EVs are larger than 100 nm, and therefore do not correspond to the so-called exosomes. This result is contrary to the basic notion underlying the use of EVs as biomarkers, according to which a vesicle originating from a cell membrane bears the same membrane antigens as its parental cell. We found also that a large amount of EVs do not expose PS, about 30% with TRAP and 20% for CRP-XL. The presence of these EVs

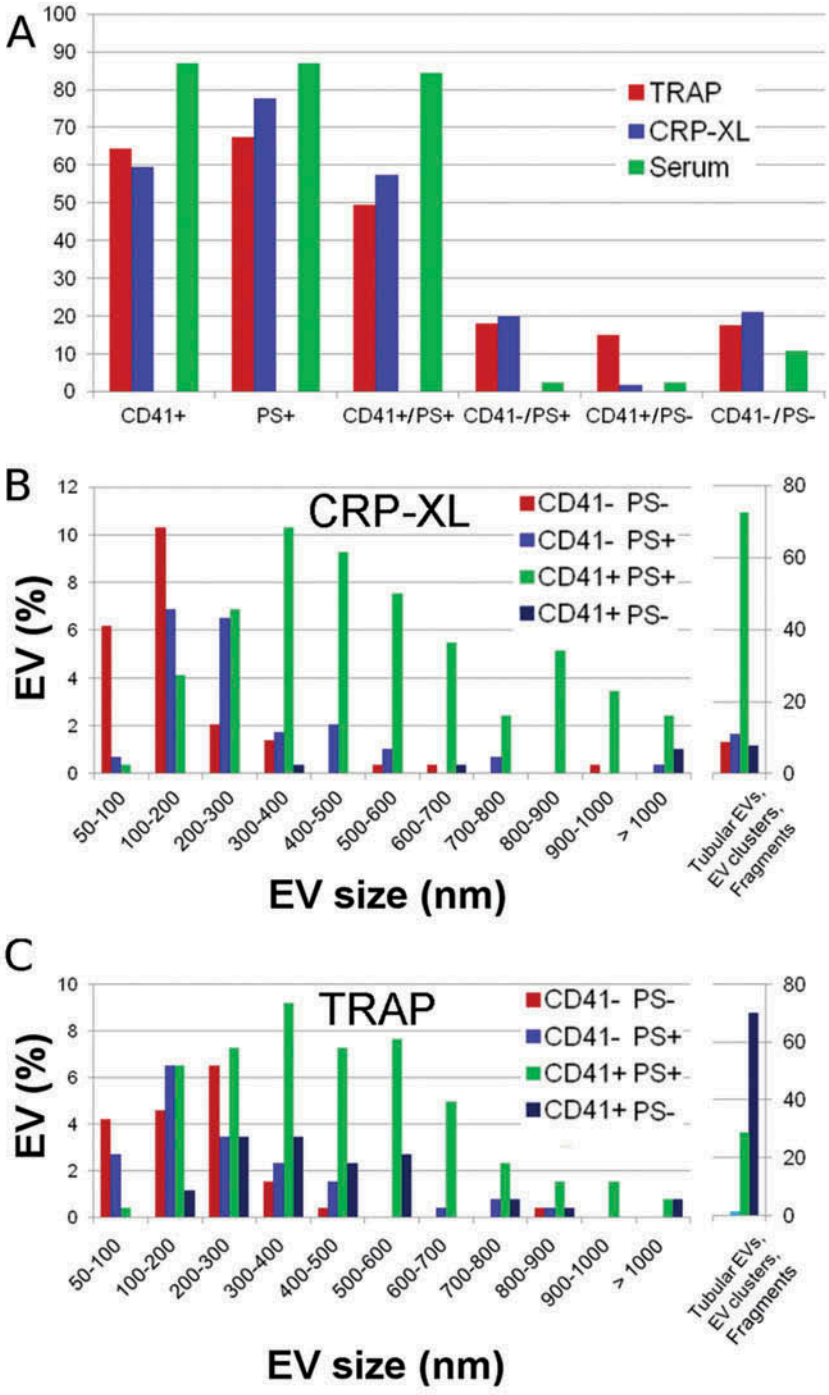

Figure 4. Phenotype of EVs from activated platelets. (A) The populations of isolated spherical EVs are grouped according to the following phenotypes (from left to right): CD41+, PS+, CD41+/PS+, CD41-/PS+, CD41+/PS-, CD41-/PS-, for TRAP (red), CRP-XL (green) and serum (yellow). (B, C) Size distribution of the various populations of EVs from platelets activated by CRP-XL (B) and TRAP (C). The right part of the graphs (from 50 nm to >1000 nm) corresponds to isolated spherical EVs, and the left part to tubular EVs, EV clusters and large fragments.

indicates that, in addition to the two main mechanisms of EV formation [6], other mechanisms must exist [37]. The small amount of CD41+/PS- EVs may correspond to EVs shed from the plasma membrane without redistribution of PS molecules, in a process symmetrically converse to endocytosis. Among those, the long pseudopods (Figure 2E) result most likely from a fragmentation of the platelet plasma membrane, similar to the long tubes of erythrocyte origin observed in the PFP samples [14]. On the other hand, CD41-/PS+ and CD41-/PS- may correspond to cytoplasmic vesicles expelled from the cytoplasm, possibly at, or close to, a site where an EV is shed. In this context, it is interesting to note that EVs containing cytoplasmic organelles like mitochondria (Figure 7A, B), α-granules (Figure 7C) or smaller EVs (Figure 7D) are occasionally observed in activated platelet samples [38]. This suggests that EVs shed from the plasma membrane may take with them the elements contained in the cytoplasm volume near the site of their formation, and are able to accommodate their size to the size of the material to cargo. It is also possible that EVs do not contain the entire protein diversity of their membrane compartment of origin. Lipids are known to diffuse faster than proteins in the membrane plane, so that protein-poor or protein-free vesicles may form during shedding. Mechanisms of active protein sorting may also take place during EV formation. Further study will be needed to elucidate the diversity of mechanisms leading to the formation of EVs.

In this context, the tubular EVs deserve a further comment. Tubular EVs present structural similarities – in diameter, length, presence of bundles of long and parallel fibers – with the

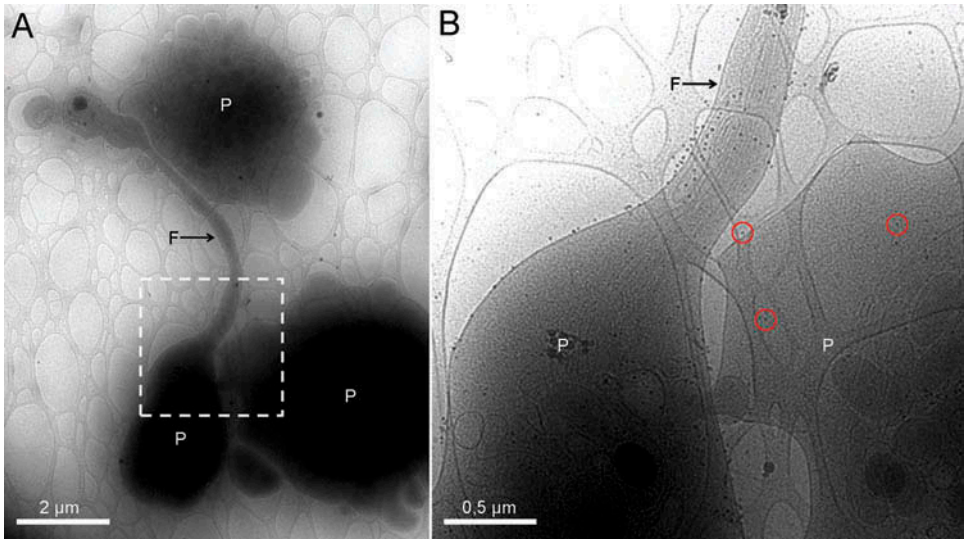

Figure 5. Activated platelet areas present higher surface density of CD41. (A) Low magnification view showing three platelets (labeled P) in a thrombin-activated sample. The platelet on the left presents a long filopodia extension (labeled F), which is a characteristic morphological change of activated platelets [40], while the two other platelets, on the bottom and top right, do not present morphological signs of activation. (B) High-magnification view of the boxed area in (A). The density of anti-CD41-gold-NPs is significantly higher on the surface of the activated platelet (left) and the filipodia (F) than on the nonactivated platelet (for clarity, several gold-NPs are marked with a red circle). Note the bundle of long fibers within the filipodia extension.

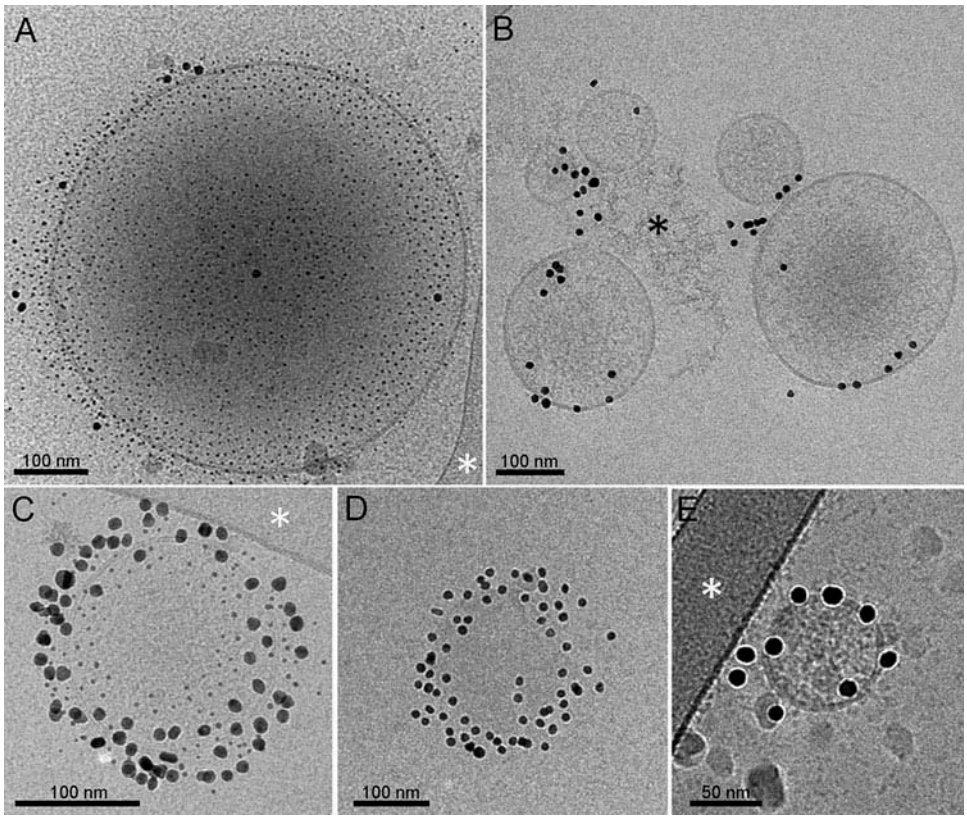

Figure 6. Characterization of CD63-positive EVs from activated platelets. (A) Large spherical EV (550 nm diameter) double labeled with 4-nm Anx5-gold-NPs and 10-nm anti-CD63-gold-NPs. Although the density of CD63 labeling is low, labeling is entirely specific as evidenced from the near-complete absence of gold-NPs in the surrounding area. (B) Cluster of five CD63-positive EVs, of size ranging from 100 to 300 nm, linked via some amorphous, non-vesicular material (black asterisk). This image is taken from a single labeling experiment with anti-CD63-gold-NPs. (C–E) Activated platelet EVs of small size, densely labeled with anti-CD63-gold-NPs. (A, B, D, E) CRP-XL activation, (C) serum.

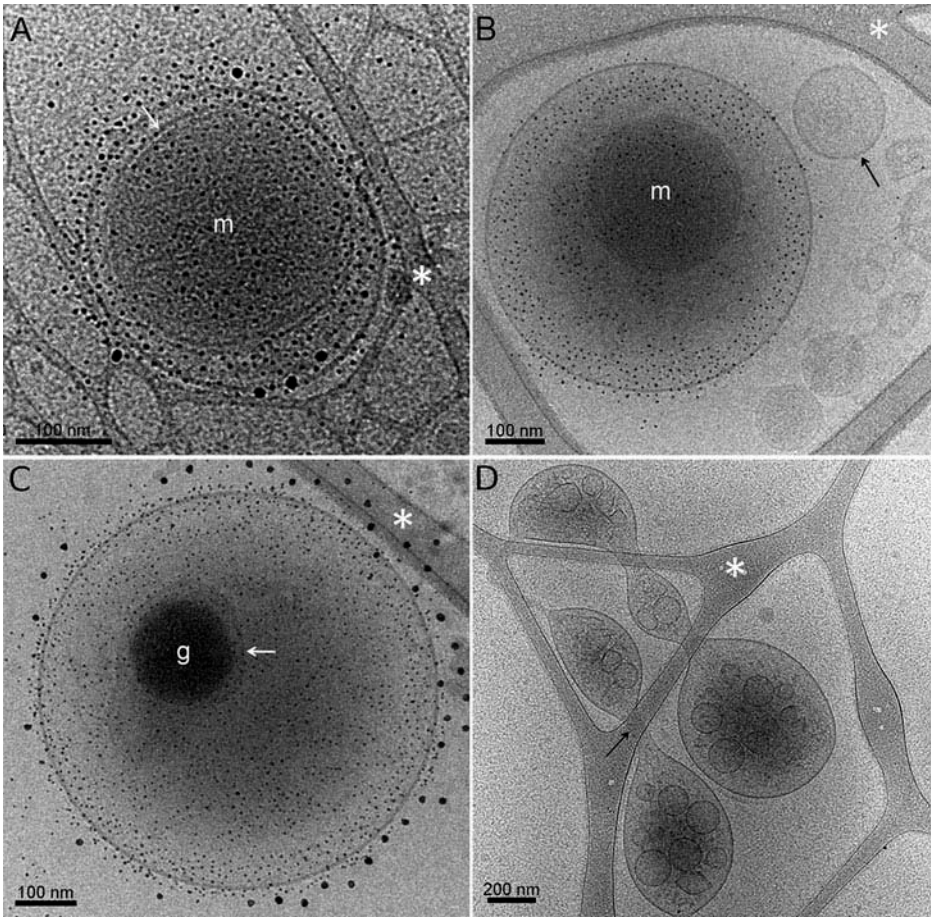

Figure 7. Large EV fragments containing organelles and cytoplasmic vesicles in activated platelet samples. (A,B) Examples of EVs containing mitochondria (M). Mitochondria are recognized by their size, around 300 nm, their high electron-scattering density, which renders them darker than the surrounding vesicular medium, and the presence of a double membrane at their periphery (white arrow in (A)). The EV in (A) is only slightly larger than the mitochondrion, while the EV in (B) is about twice larger. Some EVs are observed that contain several, up to three, mitochondria (data not shown). In Figure B, adapted from [41], CD41-/PS- EVs (arrow) are located next to the CD41-/PS+ mitochondrion-containing EV. (C) CD41+/PS+ EV containing an α-granule (g). The α-granule is characterized by its dark contrast and the presence of a surrounding membrane envelope (white arrow). (D) Large membrane fragment filled up with vesicles. The large membrane fragment is deformed suspended over the supporting carbon net, presenting deformations at contact points with the carbon threads, as expected for a soft object. This CD41-/PS- fragment looks like a bag containing a cargo of very small EVs, of diameter around 50 nm or even smaller. Note the unusual non-circular shape of some of these EVs. We hypothesize that the bag-like EV and the small EVs correspond to a multi-vesicular body containing exosomes. (A) serum; (B, C) CRP-XL activation; (D) PRP sample before activation.

filopodia extensions, which are characteristic of platelets after activation [40]. It is therefore logical to propose that tubular EVs derive from filopodia, which protrude from the platelet surface and then are shed in the external medium. The fact that tubular EVs do not expose PS implies that their formation involves a process of plasma membrane shedding without lipid scrambling.

About CD63-positive EVs

In agreement with Heijnen [1], we found that activated platelets release small EVs expressing CD63, a classical marker of exosomes [27, 28]. However, in addition to these small EVs expressing CD63 at high density, we also found that the majority of larger EVs, up to 1 μm size, expressed also CD63, yet at a significantly lower density (Figure 6). Although this result may seem unexpected, several recent studies have shown that some classically used exosomal markers were also present in non-exosomal EVs [28, 39], stressing the heterogeneity of EV preparations and the difficulty of their purification. Heijnen et al. [1] reported that, in activated platelet samples, a significant amount of CD63 was found in 10 000 g pellet, which indicates that they are associated with large EVs and not exosomes. Therefore, the presence of large EVs expressing CD63 is in keeping with these previous reports.

On the other hand, our finding that the majority of CD63-positive EVs in activated platelet samples are large EVs constitutes a novel information, as no quantitative analysis of CD63-positive EVs has been reported previously. Although the labeling density of the large EVs is significantly lower than that of the small EVs, this result draws attention on the potential pitfalls that may arise from the use of CD63 to purify exosomes, e.g. by immuno-purification.

Acknowledgments

We thank Mrs. Chaléat and the Laboratoire Mutualiste d'Analyse Médicales de Pessac for their help with the collection of blood samples. We thank Pr. Nurden for the gift of TRAP and Dr. Pasquet and Pr. Nurden for their help and advices at early stages of this study.

Funding

This study was supported by ANR (grant 11-BSV1-03501 to ARB).

Conflicts of interests

The authors declare no conflict of interest.

References

1. Heijnen HF, Schiel AE, Fijnheer R, Geuze HJ, Sixma JJ. Activated platelets release two types of membrane vesicles: microvesicles by surface shedding and exosomes derived from exocytosis of multivesicular bodies and alpha-granules. Blood 1999 Déc.;94(11):3791–3799.
2. van der Pol E, Böing AN, Harrison P, Sturk A, Nieuwland R. Classification, functions, and clinical relevance of extracellular vesicles. Pharmacol Rev 2012 Juill;64(3):676–705.
3. Zwaal RF, Schroit AJ. Pathophysiologic implications of membrane phospholipid asymmetry in blood cells. Blood 1997 Févr.;89 (4):1121–1132.
4. Morel O, Jesel L, Freyssinet J-M, Toti F. Cellular mechanisms underlying the formation of circulating microparticles. Arterioscler Thromb Vasc Biol 2011 janv.;31(1):15–26.
5. Johnstone RM. Revisiting the road to the discovery of exosomes. Blood Cells Mol Dis 2005 juin;34(3):214–219.
6. Raposo G, Stoorvogel W. Extracellular vesicles: exosomes, microvesicles, and friends. J Cell Biol 2013 Févr.;200(4):373–383.
7. Witwer KW, et al. Standardization of sample collection, isolation and analysis methods in extracellular vesicle research. J Extracell Vesicles 2013;2:20360.
8. VanWijk MJ, VanBavel E, Sturk A, Nieuwland R. Microparticles in cardiovascular diseases. Cardiovasc Res 2003 Août;59(2):277–287.
9. Théry C, Ostrowski M, Segura E. Membrane vesicles as conveyors of immune responses. Nat Rev Immunol 2009 Août;9(8):581–593.
10. Taylor DD, Gercel-Taylor C. Exosomes/microvesicles: mediators of cancer-associated immunosuppressive microenvironments. Semin Immunopathol 2011 Sept.;33(5):441–454.
11. Boilard E, et al. Platelets amplify inflammation in arthritis via collagen-dependent microparticle production. Science 2010 Janv.;327(5965):580–583.
12. Nazarenko I, Rupp A-K, Altevogt P. Exosomes as a potential tool for a specific delivery of functional molecules. Methods Mol Biol Clifton NJ 2013;1049:495–511.
13. Chandler WL, Yeung W, Tait JF. A new microparticle size calibration standard for use in measuring smaller microparticles using a new flow cytometer. J Thromb Haemost 2011; 9(6)1216–1224.
14. Arraud N, et al. Extracellular vesicles from blood plasma: determination of their morphology, size, phenotype and concentration. J Thromb Haemost JTH 2014 Mai;12(5)614–627.
15. Arraud N, Gounou C, Linares R, Brisson AR. A simple flow cytometry method improves the detection of phosphatidylserine-exposing extracellular vesicles. J Thromb Haemost JTH 2015 Févr.; 13(2):237–247.
16. Arraud N, Gounou C, Turpin D, Brisson AR. Fluorescence triggering: A general strategy for enumerating and phenotyping extracellular vesicles by flow cytometry. Cytometry A 2016;89:184–195.
17. Tait JF, Gibson DF, Smith C. Measurement of the affinity and cooperativity of annexin V-membrane binding under conditions of low membrane occupancy. Anal Biochem 2004 Juin;329(1)112–119.
18. Wolf P. The Nature and Significance of Platelet Products in Human Plasma. Br J Haematol 1967 Mai;13(3):269–288.
19. Chargaff E, West R. The biological significance of the thromboplastic protein of blood. J Biol Chem 1946 Nov.;166(1)189–197.
20. Horstman LL, Ahn YS. Platelet microparticles: a wide-angle perspective. Crit Rev Oncol Hematol 1999 avr.;30(2):111–142.
21. Gemmell CH, Sefton MV, Yeo EL. Platelet-derived microparticle formation involves glycoprotein IIb-IIIa. Inhibition by RGDS and a Glanzmann's thrombasthenia defect. J Biol Chem 1993;268 (20):14586–14589.
22. Agouti I, et al. Platelet and not erythrocyte microparticles are procoagulant in transfused thalassaemia major patients. Br J Haematol 2015; 171(4)615–624.
23. Bevers EM, Comfurius P, Zwaal RF. Changes in membrane phospholipid distribution during platelet activation. Biochim Biophys Acta 1983 Déc.;736(1)57–66.
24. Sims PJ, Wiedmer T, Esmon CT, Weiss HJ, Shattil SJ. Assembly of the platelet prothrombinase complex is linked to vesiculation of the platelet plasma membrane. Studies in Scott syndrome: an isolated defect in platelet procoagulant activity. J Biol Chem 1989; 264(29) 17049–17057.
25. Thiagarajan P, Tait JF. Collagen-induced exposure of anionic phospholipid in platelets and platelet-derived microparticles. J Biol Chem 1991;266(36):24302–243027.
26. Stuart MC, Bevers EM, Comfurius P, Zwaal RF, Reutelingsperger CP, Frederik PM. Ultrastructural detection of surface exposed phosphatidylserine on activated blood platelets. Thromb Haemost 1995 Oct.;74(4):1145–1151.
27. Escola J-M, Kleijmeer MJ, Stoorvogel W, Griffith JM, Yoshie O, Geuze HJ. Selective enrichment of tetraspan proteins on the internal vesicles of multivesicular endosomes and on exosomes secreted by human B-lymphocytes. J Biol Chem 1998; 273(32)20121–20127.
28. Kowal J, et al. Proteomic comparison defines novel markers to characterize heterogeneous populations of extracellular vesicle subtypes. Proc Natl Acad Sci USA 2016 Févr.;113(8):E968–977.
29. Thiagarajan P, Tait JF. Collagen-induced exposure of anionic phospholipid in platelets and platelet-derived microparticles. J Biol Chem 1991;266(36):24302–24307.
30. Miyazaki Y, et al. High shear stress can initiate both platelet aggregation and shedding of procoagulant containing microparticles. Blood 1996 Nov.;88(9)3456–3464.
31. Shattil SJ, Kim C, Ginsberg MH. The final steps of integrin activation: the end game. Nat Rev Mol Cell Biol 2010 Avr.;11(4):288–300.
32. Arraud N, Gounou C, Turpin D, Brisson AR. Fluorescence triggering: A general strategy for enumerating and phenotyping extracellular vesicles by flow cytoametry. Cytometry A 2016;89:184–195.
33. György B, et al. Detection and isolation of cell-derived microparticles are compromised by protein complexes resulting from shared biophysical parameters. Blood 2011 Janv.;117(4):e39–48.
34. Ashcroft BA, et al. Determination of the size distribution of blood microparticles directly in plasma using atomic force microscopy and microfluidics. Biomed Microdevices 2012 Mars;14(4):641–649.
35. Lawrie AS, Albanyan A, Cardigan RA, Mackie IJ, Harrison P. Microparticle sizing by dynamic light scattering in fresh-frozen plasma. Vox Sang 2009 Avr.;96(3):206–212.
36. Dragovic RA, et al. Sizing and phenotyping of cellular vesicles using Nanoparticle Tracking Analysis. Nanomedicine Nanotechnol Biol Med 2011 déc.;7(6):780–788.
37. Booth AM, et al. Exosomes and HIV Gag bud from endosome-like domains of the T cell plasma membrane. J Cell Biol 2006;172 (6):923–935.
38. Boudreau LH, et al. Platelets release mitochondria serving as substrate for bactericidal group IIA-secreted phospholipase a to promote inflammation. Blood 2014;124(14):2173–2183.
39. Bobrie A, Colombo M, Krumeich S, Raposo G, Thery C. Diverse subpopulations of vesicles secreted by different intracellular mechanisms are present in exosome preparations obtained by differential ultracentrifugation. J Extracell Vesicles 2012;1:18397.
40. Hartwig JH. Mechanisms of actin rearrangements mediating platelet activation. J Cell Biol 1992 Sept.;118(6):1421–1442.
41. Boilard E, Duchez A-C, Brisson A. The diversity of platelet microparticles. Curr Opin Hematol 2015;22(5):437–444.